Research Square

Preprints are preliminary reports that have not undergone peer review.
They should not be considered conclusive, used to inform clinical practice,
or referenced by the media as validated information.

APOE ε4 genotype defines divergent trajectories of microglial metabolic stress across Alzheimer's disease progression: single-nucleus transcriptomic evidence linking lipid dysregulation to cognitive decline

Sung-Hoon Yoon
Wonkwang University Hospital
Chan-Mo Yang
Wonkwang University Hospital
Sang-Yeol Lee
Wonkwang University Hospital
Dae-Jin Kim
Wonkwang University Hospital
Se Hwan Lee
Soon Chun Hyang University Cheonan Hospital
June-Woo Kim
Wonkwang University
Young Hyeon Ahn
lina824@naver.com

Soon Chun Hyang University Cheonan Hospital
Young Hyun Jung
Soonchunhyang University

Research Article

Keywords: Alzheimer disease, Microglia, APOE protein, human, Transcriptome, RNA-Seq, Lipid metabolism, Tauopathies, Cognitive dysfunction, Neuroinflammation, Single-cell gene expression analysis

Posted Date: April 27th, 2026

DOI: https://doi.org/10.21203/rs.3.rs-9401612/v1

License: This work is licensed under a Creative Commons Attribution 4.0 International License.
Read Full License

Additional Declarations: No competing interests reported.

Abstract

Background: Microglial activation is increasingly implicated in Alzheimer's disease (AD) pathophysiology, yet the cell-type specificity of glial metabolic stress responses and their relationship to tau pathology and cognitive decline remain poorly characterized. We examined whether a lipid-metabolic gene expression signature, the Metabolic Stress Score (MSS), differed across glial cell types in its association with tau burden, cognitive outcomes, and APOE ε4 genotype.

Methods: Single-nucleus RNA sequencing data from 370 ROSMAP donors (APOE ε2 carriers excluded) were analyzed. MSS was computed as a pseudobulk composite of nine lipid-metabolic genes across microglia, astrocytes, and oligodendroglia. Associations with Braak stage and MMSE were examined using linear regression adjusted for age, sex, and PMI. Glial subtype proportions and their coupling to MSS were assessed. Mediation analysis examined whether microglial MSS mediated the Braak–MMSE relationship, and APOE ε4–dependent trajectories were evaluated using a Braak × APOE4 interaction term.

Results: Among the three glial cell types, only microglial MSS was significantly associated with Braak stage ($\beta = +0.313$, $p = 0.003$) and MMSE ($\beta = -2.534$, $p = 0.002$). Microglial MSS partially mediated the Braak–MMSE relationship (indirect effect: $\beta = -0.304$, $p = 0.006$; proportion mediated: 11.1%), coupled to expansion of the lipid-droplet associated microglia (LDAM) subtype ($\beta = +0.019$, $p < 0.001$). A significant Braak × APOE4 interaction ($\beta = -0.601$, $p = 0.006$) revealed divergent trajectories: APOE ε4 carriers showed constitutively elevated MSS from early Braak stages (Braak 1: +0.490), comparable to non-carriers at Braak stages 5–6, while non-carriers showed a progressive increase. Astrocyte and oligodendroglia MSS were coupled to subtype compositional shifts but showed no significant associations with tau pathology or cognitive outcomes.

Conclusions: Microglial metabolic stress, reflected by lipid-metabolic gene dysregulation and LDAM expansion, selectively mediates the association between tau pathology and cognitive decline in AD. APOE ε4 genotype shapes this trajectory, with carriers exhibiting early-onset metabolic dysfunction independent of tau burden. These findings highlight microglial lipid metabolism as a cell-type-specific and genotype-dependent contributor to AD pathophysiology, with implications for early neuroinflammatory stratification and targeted therapeutic development.

1. Background

Alzheimer's disease (AD) is characterized by the progressive accumulation of amyloid-β plaques and neurofibrillary tau tangles, two neuropathological hallmarks that drive synaptic loss, neurodegeneration, and cognitive decline (1, 2). Although tau pathology shows stronger correlation with cognitive severity than amyloid burden alone, the cellular mechanisms by which tau accumulation translates to clinical deterioration remain incompletely understood (3). Converging evidence implicates glial dysfunction as a critical intermediary in this process: microglia, astrocytes, and oligodendroglia undergo substantial transcriptional and functional remodeling in AD, and glial activation has been correlated with both tau

pathology burden and clinical progression in postmortem and neuroimaging studies (4, 5). Microglial activation and tau propagation co-progress spatially across Braak stages in living human brain, and their co-occurrence is synergistically associated with cognitive impairment (5). However, the extent to which cell-type-specific metabolic stress contributes to these associations — and whether such contributions differ by genetic risk background — has not been systematically examined at the single-cell level.

Metabolic dysfunction is increasingly recognized as a core feature of AD pathophysiology (6). Beyond homeostatic surveillance, microglia adopt disease-associated transcriptional states (DAM) in response to amyloid and tau pathology, among which a subpopulation termed lipid-droplet accumulating microglia (LDAM) represents a particularly dysfunctional phenotype (7, 8). LDAM exhibit impaired phagocytic capacity, elevated reactive oxygen species production, and a pro-inflammatory secretory profile, and accumulate in an age-dependent manner in both mouse and human brain (9). Critically, LDAM abundance is highest in APOE ε4/ε4 AD tissue, and conditioned media from lipid droplet-rich microglia induces tau phosphorylation in human iPSC-derived neurons in an APOE-dependent manner, directly implicating microglial lipid dysregulation in downstream tau pathology (10). Beyond microglia, astrocytes undergo disease-stage-dependent transcriptional changes in AD, including reactive state transitions and dysregulation of cholesterol biosynthesis and glutamate transport that correlate with tau pathology burden (11). Oligodendrocyte lineage cells similarly adopt disease-associated states characterized by impaired myelination support and altered lipid metabolism (11–13). Whether the degree of metabolic stress across these glial lineages relates to tau pathology burden and clinical outcomes in a cell-type-specific manner, however, remains unresolved.

The APOE ε4 allele is the strongest genetic risk factor for sporadic AD (14). APOE ε4 heterozygous carriers face approximately 3–4-fold and homozygous carriers approximately 8–12-fold increased risk for AD relative to the ε3/ε3 reference genotype (14). APOE ε4 expression alters microglial lipid metabolism through impaired cholesterol efflux and lipid droplet accumulation, and drives a constitutively pro-inflammatory transcriptional state, independent of amyloid or tau burden (15, 16). The APOE ε2 allele exerts opposing protective effects through enhanced lipid efflux capacity and reduced neuroinflammatory tone, and its inclusion would introduce confounding biological effects that obscure dose-response relationships between ε4 dosage and glial metabolic stress; accordingly, APOE ε2 carriers were excluded from the present study (14).

Single-nucleus RNA sequencing (snRNA-seq) of postmortem human brain tissue offers an unprecedented opportunity to characterize glial metabolic states at cellular resolution across large, clinically well-characterized cohorts. The Religious Orders Study and Memory and Aging Project (ROSMAP) provides a particularly well-suited resource for such analyses, offering deeply phenotyped longitudinal data linked to postmortem snRNA-seq from the dorsolateral prefrontal cortex (17). Prior snRNA-seq studies of human microglia have defined disease-associated transcriptional states and their relationship to AD pathology; however, these studies have primarily focused on subtype identification rather than quantitative metabolic stress assessment, and have not examined multi-lineage glial

metabolic profiles in relation to tau staging and cognitive outcomes within a genotype-stratified framework (18, 19).

In the present study, we constructed cell-type-specific Metabolic Stress Scores (MSS) for microglia, astrocytes, and oligodendroglia using a nine-gene signature capturing key nodes of glial lipid and energy metabolism. Using data from 370 ROSMAP donors (APOE ε2 carriers excluded), we examined: (1) the associations between glial MSS and tau pathology burden (Braak stage) and cognitive performance (MMSE); (2) the relationship between MSS and glial subtype composition; (3) APOE ε4-dependent differences in microglial metabolic trajectories across Braak stages; and (4) whether microglial MSS mediates the association between tau pathology and cognitive decline.

2. Methods

2.1 Study Cohort

The Religious Orders Study and Memory and Aging Project (ROSMAP) are two longitudinal cohort studies of aging and dementia conducted at Rush University Medical Center (17). Both studies enroll older adults without known dementia at baseline and follow participants annually until death, with brain donation upon death. As this study utilized de-identified, publicly available data from the ROSMAP cohort (accessible via the AD Knowledge Portal, syn18485175) (20),, the study was reviewed and granted exemption by the Institutional Review Board of Soonchunhyang University Cheonan Hospital (IRB No. SCHCA 2026-03-029). The original ROSMAP studies were approved by the Rush University Medical Center Institutional Review Board, and all participants provided written informed consent prior to enrollment.

For the present study, we analyzed single-nucleus RNA sequencing (snRNA-seq) data from 449 ROSMAP participants with available postmortem brain tissue (dorsolateral prefrontal cortex). After filtering for participants with complete data on all variables of interest — including Mini-Mental State Examination (MMSE) score, Braak neurofibrillary tangle stage, age at death, sex, post-mortem interval (PMI), and APOE genotype — and excluding donors carrying the APOE ε2 allele (ε2/ε2, ε2/ε3, ε2/ε4; n = 76) and donors with missing data on key covariates (Braak stage, n = 1; APOE genotype, n = 1; post-mortem interval, n = 1), the final analytic sample comprised 370 participants (APOE ε4 carriers: n = 109; non-carriers: n = 261). **(**Fig. 1**)**

2.2 Single-nucleus RNA Sequencing Data Processing

Pre-processed snRNA-seq data were obtained from the AD Knowledge Portal (syn18485175) (20). Briefly, nuclei were isolated from the dorsolateral prefrontal cortex and sequenced using the 10x Genomics Chromium platform. Quality control was performed in the original study using the Seurat framework, including exclusion of nuclei with fewer than 200 detected genes and removal of low-quality nuclei based on mitochondrial read proportions (20); normalization and dimensionality reduction were performed using SCTransform (21, 22). For the present analysis, cell-type-specific expression matrices

were extracted from archived h5Seurat objects containing microglia (n = 86,612 nuclei), astrocytes (n = 228,925 nuclei), and oligodendroglia (n = 409,572 nuclei). For microglial analyses, additional quality filtering was applied: nuclei identified as putative doublets (DoubletFinder score > 0.5; n = 1,541) and non-microglial contaminating populations (Macrophages, n = 2,070; Monocytes, n = 813) were excluded, retaining 82,380 microglial nuclei for downstream analysis.

2.3 Cell Type Annotation

Microglial subclusters were identified through unsupervised clustering and annotated based on established marker gene expression profiles (18, 19). Cluster identity was determined by examining the mean expression of canonical marker genes across all subclusters. The IFN-responsive microglial state was defined by high expression of interferon-stimulated genes (IRF7, ISG15, MX1, IFIT1, STAT1) (18). The lipid-droplet accumulating microglia (LDAM) state was characterized by upregulation of lipid metabolism genes (LPL, APOE, TREM2, SPP1, GPNMB) and downregulation of homeostatic markers (P2RY12, TMEM119, CX3CR1) (9). Homeostatic microglia were defined by high expression of P2RY12, TMEM119, and CX3CR1 (7). For astrocytes, A1 reactive astrocytes were identified by elevated SERPINA3, CD44, and GFAP expression (23). For oligodendroglia, subclusters were classified as oligodendrocyte precursor cells (OPC), transitional cells, and mature oligodendrocytes based on expression of PDGFRA, BCAS1, and MBP respectively (13). Subtype proportions were calculated as the fraction of each subtype relative to the total cell count per donor **(Supplementary Table 3)**. Microglial subtype annotations are illustrated in Supplementary Figs. 4 and 6; annotations for astrocytes and oligodendroglia are shown in Supplementary Fig. 5.

2.4 Metabolic Stress Score (MSS) Construction

To quantify cellular metabolic dysfunction at the donor level, we developed a Metabolic Stress Score (MSS) for each cell type. Nine genes were selected as MSS components based on their established roles in glial metabolic homeostasis and lipid handling: HK2 and LDHA (aerobic glycolysis and lactate metabolism, upregulated in disease-associated microglia), GYS1 (glycogen metabolism in reactive astrocytes), ABCA1 and ABCG1 (cholesterol efflux transporters, implicated in TREM2-dependent microglial lipid homeostasis), APOE and LPL (lipid transport, hallmark genes of the LDAM state), PPARG (master regulator of lipid metabolism in glia), and ELOVL5 (fatty acid elongation, involved in membrane lipid remodeling under metabolic stress) (9, 10, 24–26). This gene set was curated de novo based on convergent evidence from studies of disease-associated microglia and glial lipid dysfunction; no pre-existing composite MSS has been previously reported.

For each donor, mean normalized expression of each MSS gene was calculated across all nuclei of the relevant cell type using SCTransform-normalized counts

(22). Gene-level expression values were then z-scored across donors to standardize for differences in gene-level variance. The MSS was computed as the mean of the nine z-scored gene values. To verify directional consistency, Pearson correlations between individual gene z-scores and Braak stage were examined across donors. Seven of nine genes showed positive correlations with Braak stage (r = 0.074–

0.257), consistent with upregulation of lipid-metabolic stress pathways in advanced AD pathology. Two genes (GYS1, r = 0.008; ELOVL5, r = − 0.099) showed minimal or weakly inverse correlations; given their established roles in glial glycogen metabolism and fatty acid elongation respectively, and the small magnitude of deviation, these genes were retained in the composite score without materially affecting overall MSS directionality. Higher MSS values therefore reflect greater expression of lipid-metabolic stress genes, consistent with the activated but dysfunctional metabolic phenotype observed in disease-associated glia. To assess cell-type specificity, this procedure was applied independently to microglia, astrocytes, and oligodendroglia; results for astrocytes and oligodendroglia are presented in Supplementary Materials (Supplementary Fig. 1).

2.5 Clinical and Pathological Variables

Clinical and pathological data were obtained from the ROSMAP clinical dataset (syn3157322) (17). Cognitive function was assessed using the Mini-Mental State Examination (MMSE), with the last valid score used as the primary cognitive outcome. Neurofibrillary tangle burden was quantified using Braak staging (0–6) (27), determined by neuropathological assessment of postmortem brain tissue. APOE genotype was determined by high-throughput sequencing (28) and donors were classified as APOE ε4 carriers (genotypes 34 or 44) or non-carriers (genotype 33). Donors carrying the APOE ε2 allele (genotypes 2/2, 2/3, or 2/4) were excluded from primary analyses due to the distinct neuroprotective effects of ε2 on AD pathology (n = 76 excluded; ε2/ε2: n = 5, ε2/ε3: n = 64, ε2/ε4: n = 7), yielding a final analytic sample of 370 donors. Age at death was used as the primary demographic covariate; participants with age recorded as "90+" were assigned a value of 90 years. Additional covariates included sex and post-mortem interval (PMI, hours).

2.6 Statistical Analysis

All statistical analyses were performed in R (version 4.3.1). Group differences in demographic and clinical characteristics between APOE ε4 carriers and non-carriers were assessed using independent samples t-tests for continuous variables and chi-square tests for categorical variables.

Gene Set Enrichment Analysis. To characterize pathway-level transcriptional changes across glial cell types, GSEA was performed on pseudobulk differentially expressed genes for microglia, astrocytes, and oligodendroglia using the fgsea R package against the MSigDB Hallmark and Reactome gene set collections (29–32). Normalized enrichment scores (NES) and false discovery rates (FDR) were calculated; pathways with FDR < 0.05 were considered statistically significant. **(Supplementary Table 1–2)**

MSS-cognitive coupling. The association between microglial MSS and cognitive function was examined using multiple linear regression with MMSE as the dependent variable and microglial MSS as the primary predictor, adjusting for age at death, sex, and PMI. Identical models were fitted for astrocytes and oligodendroglia to assess cell-type specificity; these results are presented in **Supplementary Fig. 2**, Table 1

Table 1. Participant Characteristics by APOE ε4 Status			
	APOE ε4− (n=261)	**APOE ε4+ (n=109)**	**p-value**
Demographics			
Age at death, years	86.7 ± 4.5	87.1 ± 4.1	0.414
Sex, % male	34.1%	34.0%	0.966
PMI, hours	7.9 ± 5.0	7.6 ± 4.8	0.628
Disease Severity			
MMSE (last valid)	22.7 ± 7.7	18.1 ± 10.1	< 0.001
Braak stage	3.38 ± 1.18	4.06 ± 1.17	< 0.001
Metabolic Stress Score			
$MSS^{microglia}$	−0.04 ± 0.52	0.09 ± 0.57	0.038*
MSS	−0.02 ± 0.51	0.01 ± 0.59	0.625
$MSS^{oligodendroglia}$	0.02 ± 0.66	−0.02 ± 0.67	0.965

Values are mean ± SD unless otherwise stated. p-values from independent t-test or chi-square test. *p < 0.05.

Braak trajectory analysis. To examine the relationship between tau pathology progression and glial metabolic stress, linear regression was performed with MSS as the dependent variable and Braak stage as the primary predictor, adjusting for age at death, sex, and PMI. This analysis was conducted independently for microglia, astrocytes, and oligodendroglia.

APOE ε4-dependent trajectory. To examine whether APOE ε4 genotype modifies the relationship between Braak stage and microglial MSS, a Braak × APOE4 interaction term was included in a linear regression model adjusting for age at death, sex, and PMI. To further characterize genotype-stratified MSS levels across Braak stages, mean MSS values were compared between APOE ε4 carriers and non-carriers at each Braak stage.

Glial subtype coupling. The associations between cell-type-specific MSS and glial subtype proportions (microglial LDAM and IFN-responsive subtypes; astrocyte A1 reactive subtype; oligodendroglial OPC and mature oligodendrocyte subtypes) were examined using linear regression, adjusting for age at death, sex, PMI, and APOE ε4 status.

Mediation analysis. To test whether microglial metabolic stress mediates the relationship between tau pathology and cognitive decline, formal mediation analysis was conducted using the mediation R package (33). The indirect effect (Braak → microglial MSS → MMSE) was estimated using bias-

corrected bootstrap confidence intervals (1,000 iterations). The proportion of the total effect mediated by microglial MSS was calculated as the ratio of the indirect effect to the total effect.

A two-sided significance threshold of $p < 0.05$ was applied throughout. For all primary analyses, effect sizes are reported as unstandardized regression coefficients (β) with 95% confidence intervals.

3. Results

Microglial MSS was selectively elevated with advancing Braak stage and associated with lower MMSE scores, effects not observed in astrocytes or oligodendroglia. APOE ε4 carriers showed constitutively elevated microglial MSS across all Braak stages, with a significant Braak × APOE ε4 interaction. Microglial MSS partially mediated the association between tau pathology and cognitive decline (ACME = − 0.304, $p = 0.006$), accounting for 11.1% of the total effect.

3.1 Participant Characteristics

A total of 370 participants met inclusion criteria and were included in the final analysis (Fig. 1). Of the 449 donors with available snRNA-seq data, 79 were excluded due to missing clinical data (n = 3) or APOE ε2 carrier status (n = 76), yielding a final analytic sample of 370 participants (APOE ε4 carriers: n = 109; non-carriers: n = 261). Demographic and clinical characteristics are summarized in Table 1. APOE ε4 carriers and non-carriers were well-matched for age at death (87.1 ± 4.1 vs. 86.7 ± 4.5 years, $p = 0.414$), sex (34.0% vs. 34.1% male, $p = 0.966$), and PMI ($p = 0.628$). As expected, APOE ε4 carriers showed significantly lower MMSE scores (18.1 ± 10.1 vs. 22.7 ± 7.7, $p < 0.001$) and higher Braak stages (4.06 ± 1.17 vs. 3.38 ± 1.18, $p < 0.001$) compared to non-carriers. Among MSS values, microglial MSS differed significantly between APOE ε4 carriers and non-carriers ($p = 0.038$), whereas astrocyte ($p = 0.625$) and oligodendroglia ($p = 0.965$) MSS did not. Microglial subtype annotation is illustrated in **Supplementary Fig. 4**, and glial subtype annotation across all three cell types is shown in **Supplementary Fig. 5**.

3.2 Cell-type Specific Pathway Suppression in Alzheimer's Disease

GSEA revealed distinct patterns of transcriptional suppression across glial cell types, with microglia showing the most extensive and biologically coherent pathway dysregulation (Supplementary Table 1–2). In microglia, 14 Hallmark and 60 Reactome pathways were significantly suppressed (FDR < 0.05), with no pathways showing significant upregulation. Suppressed pathways clustered into two broad categories: immune effector functions, including Complement (NES=-2.01, FDR < 0.001), Inflammatory Response (NES=-1.96, FDR < 0.001), TNFα Signaling via NFκB (NES=-1.95, FDR < 0.001), and Interferon Gamma Response (NES=-1.90, FDR < 0.001); and metabolic regulation, including Cholesterol Homeostasis (NES=-1.70, FDR = 0.006) and PI3K-AKT-mTOR Signaling (NES=-1.52, FDR = 0.028). Notably, all nine MSS genes appeared exclusively within negatively enriched pathways across both gene set collections (NES range: -1.22 to -1.70), with LPL and PPARG identified among the leading-edge genes of the Cholesterol Homeostasis pathway.

Astrocytes showed a distinct suppression profile centered on cellular stress responses and energy metabolism, including TNFα Signaling via NFκB (NES=-2.16, FDR < 0.001), mTORC1 Signaling (NES=-1.98, FDR < 0.001), Hypoxia (NES=-1.90, FDR < 0.001), and Glycolysis (NES=-1.53, FDR = 0.011). Oligodendroglia showed minimal transcriptional dysregulation, with only two Hallmark pathways reaching significance and no significant Reactome pathways. The breadth and biological coherence of pathway suppression was therefore most pronounced in microglia, particularly within immune effector and lipid metabolic functions.

3.3 Microglial Metabolic Stress is Selectively Associated with Tau Pathology and Cognitive Decline

To quantify donor-level metabolic dysfunction, we computed cell-type-specific MSS values for microglia, astrocytes, and oligodendroglia. In linear regression adjusted for age at death, sex, PMI, and APOE ε4 status, higher Braak stage was significantly associated with greater microglial metabolic stress (β = 0.313, 95% CI [0.106, 0.521], p = 0.003), indicating progressive accumulation of microglial metabolic dysfunction with advancing neurofibrillary tangle pathology. Higher microglial MSS was in turn significantly associated with lower MMSE scores (β=−2.534, 95% CI [− 4.132, − 0.937], p = 0.002), indicating that greater microglial metabolic stress was associated with worse cognitive function. Neither association was significant for astrocytes (Braak: β = 0.041, p = 0.698; MMSE: β=−1.137, p = 0.164) or oligodendroglia (Braak: β = 0.052, p = 0.546; MMSE: β=−0.577, p = 0.382), further supporting the selective vulnerability of microglia to tau-associated metabolic stress and its downstream cognitive consequences (Fig. 2, Table 2).

Table 2
Cell-Type Specific Associations of MSS with Cognitive Decline and Tau Pathology

	β	95% CI	p-value
MSS ~ MMSE (cognitive decline)			
Microglia	−2.534	[− 4.132, − 0.937]	0.002*
Astrocyte	−1.137	[− 2.742, 0.468]	0.164
Oligodendroglia	−0.577	[− 1.882, 0.729]	0.382
MSS ~ Braak stage (tau pathology)			
Microglia	+ 0.313	[0.106, 0.521]	0.003*
Astrocyte	+ 0.029	[− 0.164, 0.246]	0.698
Oligodendroglia	+ 0.052	[− 0.119, 0.224]	0.546
APOE ε4 × Braak interaction (MSS outcome)			
Microglia (interaction term)	−0.601	[− 1.033, − 0.170]	0.006*
All models adjusted for age at death, sex, PMI, and APOE ε4 status. *p < 0.05.			

3.4 APOE ε4-Dependent Microglial Metabolic Stress Trajectory

To examine whether the relationship between tau pathology and microglial metabolic stress differed by APOE ε4 genotype, we tested a Braak × APOE4 interaction term in linear regression. The interaction was statistically significant (β = −0.601, 95% CI [− 1.033, − 0.170], p = 0.006), indicating that APOE ε4 genotype significantly modifies the trajectory of microglial metabolic stress across Braak stages.

APOE ε4 carriers demonstrated constitutively elevated microglial MSS across all Braak stages (APOE4 main effect: β = +0.604, p < 0.001). Mean MSS in APOE ε4 carriers at Braak stage 1 (+ 0.490) was comparable to that observed in non-carriers at Braak stages 5–6 (+ 0.204 and + 0.464, respectively), suggesting that carriers maintain a high level of microglial metabolic stress from the earliest stages of tau pathology. In contrast, non-carriers showed a progressive increase in MSS with advancing tau pathology, from − 0.109 at Braak stage 1 to + 0.464 at Braak stage 6. These divergent trajectories are illustrated in Fig. 3, **Supplementary Table 4**.

3.5 Microglial Metabolic Stress Drives Subtype Shifts and Mediates Tau-Associated Cognitive Decline

To examine whether glial metabolic stress was reflected in subtype compositional changes, we tested associations between cell-type-specific MSS and glial subtype proportions. In microglia, higher MSS was

significantly associated with greater LDAM proportion (β = 0.019, 95% CI [0.010, 0.028], p < 0.001), and LDAM proportion was in turn associated with greater tau pathology burden (β = 6.490, 95% CI [4.115, 8.865], p < 0.001) and lower MMSE scores (β=−42.61, 95% CI [− 61.14, − 24.08], p < 0.001). No significant association was observed between microglial MSS and IFN-responsive microglial proportion (β < 0.001, p = 0.975). In astrocytes, higher MSS showed a trend toward greater reactive astrocyte proportion (β = 0.043, p = 0.077); however, reactive astrocyte proportion did not associate with Braak stage or MMSE after covariate adjustment. In oligodendroglia, higher MSS was associated with greater OPC proportion (β = 0.038, p < 0.001) and lower mature oligodendrocyte proportion (β=−0.040, p < 0.001), though neither proportion associated with Braak stage or MMSE (Fig. 4, Table 3, Supplementary Fig. 2).

Table 3
Glial Subtype Coupling and Mediation Analysis

	β	95% CI	p-value
Subtype Proportion ~ MSS			
LDAM ~ $MSS^{microglia}$	+ 0.019	[0.010, 0.028]	< 0.001**
IFN-responsive ~ $MSS^{microglia}$	< 0.001	[− 0.004, 0.091]	0.944
A1 Reactive ~ MSS††	+ 0.043	[0.009, 0.095]	0.077
OPC ~ $MSS^{oligodendroglia}$	+ 0.038	[0.027, 0.050]	< 0.001**
Mature OL ~ $MSS^{oligodendroglia}$	−0.040	[− 0.051, − 0.028]	< 0.001**
LDAM ~ Disease Severity			
LDAM ~ Braak	+ 6.490	[4.115, 8.865]	< 0.001
LDAM ~ MMSE	−42.61	[− 61.14, − 24.08]	< 0.001**
Mediation Analysis: Braak → MSS → MMSE			
Total effect (Braak → MMSE)	−2.731	[− 3.472, − 2.023]	< 0.001**
Direct effect (ADE)	−2.426	[− 3.145, − 1.699]	< 0.001**
Indirect effect (ACME)	−0.304	[− 0.644, − 0.076]	0.006*
Proportion mediated	11.1%	[2.6%, 23.3%]	0.006*

†A1 reactive astrocyte proportion showed a trend toward association with astrocyte MSS (p = 0.077) but did not associate with Braak stage or MMSE. All models adjusted for age at death, sex, PMI, and APOE ε4 status. Mediation analysis based on nonparametric bootstrap (1000 simulations).

To test whether microglial metabolic stress mediates the relationship between tau pathology and cognitive decline, we conducted formal mediation analyses with Braak stage as the treatment variable,

cell-type-specific MSS as the mediator, and MMSE as the outcome. The total effect of Braak stage on MMSE was significant across all models (β=−2.731, 95% CI [− 3.472, − 2.023], p < 0.001). Only microglial MSS showed a statistically significant indirect effect (ACME = − 0.304, 95% CI [− 0.644, − 0.076], p = 0.006), mediating 11.1% (95% CI [2.6%, 23.3%]) of the total effect. The direct effect of Braak stage on MMSE remained significant after accounting for microglial MSS (β=−2.426, 95% CI [− 3.145, − 1.699], p < 0.001). Neither astrocyte MSS (ACME = − 0.029, p = 0.388) nor oligodendrocyte MSS (ACME = − 0.006, p = 0.790) showed significant mediation effects (Table 3).

4. Discussion

The present study examined metabolic stress across three major glial cell types in a large postmortem cohort of 370 ROSMAP donors. Among microglia, astrocytes, and oligodendroglia, only microglial MSS demonstrated robust associations with Braak staging and MMSE, with these effects mediated in part through expansion of the LDAM subtype. The trajectory of microglial MSS across Braak stages differed markedly by APOE ε4 status, with carriers showing an earlier metabolic ceiling that persisted across advanced tau pathology stages. In contrast, astrocyte and oligodendroglia MSS were coupled to subtype composition shifts but showed no significant associations with clinical or neuropathological outcomes, suggesting that metabolic stress responses in these cell types reflect broader glial state changes not specific to AD progression.

4.1. Microglial metabolic stress and LDAM in Alzheimer's disease

Microglial MSS was significantly associated with both Braak staging and MMSE scores, and these associations were largely driven by expansion of the LDAM subtype. This finding aligns with growing evidence that lipid droplet accumulation represents a pathologically relevant microglial state in the aging and AD brain. LDAM have been characterized as a dysfunctional, pro-inflammatory population defined by impaired phagocytosis, elevated reactive oxygen species, and increased secretion of inflammatory cytokines, accumulating in an age-dependent manner in both mouse and human brain (9). More recently, LDAM abundance was shown to be highest in APOE4/4 AD brain tissue, with conditioned media from lipid droplet-rich microglia inducing tau phosphorylation in human iPSC-derived neurons in an APOE-dependent manner (10), directly linking microglial lipid dysregulation to downstream tau pathology. Consistent with these findings, the MSS gene signature employed in the present study captures key nodes of this dysregulation, including LPL and PPARG, which regulate lipid uptake and fatty acid oxidation in microglia, and APOE itself, which mediates cholesterol transport and is upregulated in metabolically stressed microglial states (7, 34). The observed mediation of the Braak–MMSE relationship through microglial MSS, though modest in effect size (11.1%), is consistent with the upstream role proposed for microglial activation in AD-related cognitive decline. A prior analysis of ROSMAP cortical tissue similarly reported that morphologically activated microglia mediated the

association between tau pathology and cognitive decline, supporting the notion that neuroinflammatory signals, while not the dominant driver, contribute meaningfully to the tau-to-cognition pathway (35).

4.2 APOE ε4-dependent metabolic trajectory of microglial stress

APOE ε4 carriers demonstrated a distinct pattern of microglial metabolic stress across Braak stages, characterized by constitutively elevated MSS from the earliest stages of tau pathology. As shown in the group-level data, mean MSS in APOE ε4 carriers at Braak stage 1 (+ 0.490) was comparable to that observed in non-carriers at Braak stages 5–6, suggesting that APOE ε4 expression drives microglial metabolic dysfunction independently of tau burden. The significant APOE4 main effect ($\beta = +0.604$, $p < 0.001$) alongside a negative Braak × APOE4 interaction ($\beta = -0.601$, $p = 0.006$) indicates that while carriers begin at a higher baseline, the incremental increase in MSS with advancing tau pathology is attenuated relative to non-carriers, who show a more pronounced progressive trajectory.

This pattern is consistent with evidence that APOE ε4 expression drives microglial lipid droplet accumulation independently of amyloid or tau pathology (15), and that APOE ε4 microglia exhibit a constitutively pro-inflammatory transcriptional profile with impaired homeostatic gene expression even in the absence of pathological stimuli (10). Together, these findings suggest that in APOE ε4 carriers, microglial metabolic stress may be established early through genotype-driven mechanisms, with non-carriers showing a more reactive pattern in which metabolic dysfunction escalates in response to accumulating tau pathology. It should be noted that the number of APOE ε4 carriers at Braak stages 0–2 was limited (n = 12), and these early-stage estimates should therefore be interpreted with caution. Replication in larger cohorts with adequate early-stage representation will be necessary to confirm this proposed model.

4.3 Astrocyte and oligodendroglia: MSS coupling without clinical translation

In contrast to microglia, astrocyte and oligodendroglia MSS were associated with shifts in subtype composition but showed no significant associations with Braak staging or MMSE scores. For astrocytes, the expansion of reactive subtypes showed a trend toward coupling with metabolic stress ($p = 0.077$) yet remained independent of tau pathology stage and cognitive performance. This pattern may reflect an aging-driven reactive state rather than an AD-specific response. Prior work has demonstrated that normal aging induces an A1-like reactive astrocyte phenotype through microglial signaling, independent of overt neuropathology (23). Furthermore, a large-scale snRNA-seq study of 628,943 astrocytes across five cortical regions demonstrated that shifts between homeostatic and reactive astrocyte proportions occur primarily along a spatial axis, with certain subclusters showing no consistent relationship with Braak stage (11), a finding that closely parallels our observation of Braak-independent reactive astrocyte expansion. It should also be noted that astrocyte subtype annotation in snRNA-seq datasets remains challenging, with limited cross-study reproducibility and potential dilution of spatially confined pathological responses in bulk pseudobulk analyses (13).

For oligodendroglia, metabolic stress was associated with a compositional shift toward progenitor-enriched states at the expense of mature subtypes, yet this change did not translate to associations with clinical or neuropathological outcomes. Emerging evidence suggests that disease-associated oligodendrocyte states are not specific to AD pathology but may reflect a broader response to CNS damage, having been identified across multiple neurodegenerative conditions including multiple sclerosis and aging (12). Inconsistencies in the detection of reactive oligodendrocyte populations in human AD snRNA-seq datasets further complicate interpretation (8), and the functional significance of progenitor-skewed oligodendroglial composition in the context of metabolic stress remains to be established.

4.4 Translational implications and future directions

The present findings carry several translational observations, with the important caveat that causal inference is not possible from postmortem cross-sectional transcriptomic data. Most directly, the identification of LDAM expansion as a partial mediator of the Braak–MMSE relationship provides human single-cell transcriptomic evidence positioning microglial lipid droplet dynamics as a mechanistic node in AD-related cognitive decline. Prior experimental work has demonstrated that conditioned media from lipid droplet-rich microglia induces tau phosphorylation and neuronal apoptosis in an APOE-dependent manner, and that these functional deficits are attenuated when lipid droplet biogenesis is inhibited (10). The present findings extend this experimental evidence to human postmortem tissue at scale, supporting the translational relevance of microglial lipid dysregulation as a potential intervention point in AD pathophysiology, while acknowledging that the functional consequences of LDAM expansion and their amenability to modulation in human disease require direct experimental validation.

The APOE ε4–dependent trajectory of microglial MSS has additional implications for the timing of potential interventions. The observation that microglial metabolic stress appears elevated in APOE ε4 carriers already at early Braak stages is consistent with experimental evidence that APOE ε4 drives microglial lipid accumulation and a pro-inflammatory transcriptional state in an aging-dependent but pathology-independent manner (15, 36). This pattern suggests that microglial metabolic dysregulation in APOE ε4 carriers may not await advanced tau pathology, supporting the rationale for early stratification of this population in neuroinflammatory biomarker and intervention studies. Consistent with this interpretation, independent clinical evidence from a dementia trial-ready registry has demonstrated that the association between liver–metabolic stress and late-life cognitive vulnerability is amplified in an APOE ε4 dose-dependent manner (37), suggesting that the metabolic susceptibility of APOE ε4 carriers may extend across both systemic and central compartments.

Finally, the cell-type specificity of the clinical associations observed here — whereby microglial MSS, but not astrocyte or oligodendroglia MSS, was robustly associated with tau pathology and cognitive outcomes — adds to a growing body of single-cell transcriptomic evidence implicating microglia as the glial cell type most directly coupled to AD clinical progression (18, 19). This selectivity has implications for the design of targeted neuroinflammatory interventions, as it suggests that broad glial anti-inflammatory strategies may be insufficient, and that microglial-specific, and potentially lipid

metabolism–directed, approaches warrant preferential investigation. Whether the microglial metabolic stress signature identified here is amenable to modulation by existing or emerging therapeutic agents remains an open question that motivates future mechanistic and interventional research.

5 Limitations

Several limitations of the present study warrant consideration. First, the cross-sectional postmortem design precludes causal inference; the observed associations between microglial MSS, tau pathology, and cognitive decline cannot establish directionality, and reverse causation — whereby advancing neurodegeneration drives microglial metabolic stress rather than the converse — cannot be excluded. Second, the MSS was derived from pseudobulk gene expression averaged across all microglial nuclei per donor, which may obscure spatially or subtype-restricted metabolic stress signals (38). Single-cell resolution analyses and spatially resolved transcriptomics will be necessary to determine whether the MSS signal is uniformly distributed across microglial subpopulations or concentrated within specific pathological niches. Third, APOE ε4 carriers at early Braak stages were limited in number (n = 12 at Braak 0–2), and the characterization of constitutively elevated microglial MSS in this group should therefore be interpreted with caution pending replication in larger cohorts with adequate early-stage representation. Fourth, MMSE, while widely used, is an imperfect proxy for cognitive decline and may not capture the full spectrum of AD-related cognitive impairment; future studies incorporating more granular neuropsychological batteries or longitudinal cognitive trajectories would strengthen the clinical relevance of the findings (39). Fifth, while the MSS gene panel was selected based on established biological rationale, it represents a targeted rather than unbiased approach to capturing microglial metabolic dysfunction, and alternative gene signatures may yield complementary or divergent findings. Finally, all analyses were conducted in dorsolateral prefrontal cortex, and the generalizability of the present findings to other brain regions with distinct glial compositions and pathological vulnerabilities remains to be established.

6. Conclusion

The present study provides large-scale single-nucleus transcriptomic evidence that microglial metabolic stress, as captured by a lipid-metabolic gene expression signature, is selectively coupled to tau pathology burden and cognitive decline in the aging human brain. Among the three glial cell types examined, only microglial MSS demonstrated robust associations with both Braak staging and MMSE, with these effects partially mediated through expansion of the LDAM subtype — a finding that positions microglial lipid dysregulation as a mechanistically relevant node in the tau-to-cognition pathway. The APOE ε4–dependent trajectory of microglial MSS further indicates that genotype-driven metabolic dysfunction precedes advanced tau pathology in carriers, supporting the rationale for early neuroinflammatory stratification of this high-risk population. In contrast, astrocyte and oligodendroglia MSS were coupled to subtype compositional shifts but remained dissociated from clinical and neuropathological outcomes, suggesting that glial metabolic stress responses are not uniformly translated into disease-relevant signals across cell types. Together, these findings advance the

understanding of cell-type-specific glial contributions to AD pathophysiology and highlight microglial lipid metabolism as a priority target for biomarker development and therapeutic investigation in Alzheimer's disease.

Declarations

Ethics approval and consent to participate This study utilized de-identified, publicly available data from the ROSMAP cohort. The study was reviewed and granted exemption by the Institutional Review Board of Soonchunhyang University Cheonan Hospital (IRB No. SCHCA 2026-03-029). The original ROSMAP studies were approved by the Rush University Medical Center Institutional Review Board, and all participants provided written informed consent.

Consent for publication Not applicable.

Ethics approval and consent to participate This study utilized de-identified, publicly available data from the ROSMAP cohort (AD Knowledge Portal, Synapse ID: syn18485175). The study was reviewed and granted exemption by the Institutional Review Board of Soonchunhyang University Cheonan Hospital (IRB No. SCHCA 2026-03-029). The original ROSMAP studies were approved by the Rush University Medical Center Institutional Review Board, and all participants provided written informed consent prior to enrollmen

Availability of data and materials The ROSMAP single-nucleus RNA sequencing data and clinical metadata analyzed in the present study are available through the AD Knowledge Portal (https://adknowledgeportal.synapse.org; Synapse ID: syn18485175) under data use agreement.

Competing interests The authors declare that they have no competing interests.

Funding This work was supported by the National Research Foundation of Korea (NRF) grants funded by the Korea government (MSIT) (RS-2025-00555459) and by the Ministry of Education through the Global – Learning & Academic research institution for Master's·PhD students, and Postdocs (G-LAMP) Program (RS-2025-25441283). This research was supported by Soonchunhyang University Research Fund.

Authors' contributions SHY conceptualized and designed the study, performed all bioinformatic and statistical analyses, visualized the data, and wrote the original draft. CMY and SYL contributed to the interpretation of results and critically revised the manuscript. DJK contributed to the bioinformatic methodology and data curation. SHL contributed to data curation and validation. JWK contributed to the computational methodology and data processing. YHA supervised the study, contributed to data interpretation, and critically revised the manuscript. YHJ supervised the study, contributed to the study design and data interpretation, and critically revised the manuscript. All authors read and approved the final manuscript.

Acknowledgements Not applicable.

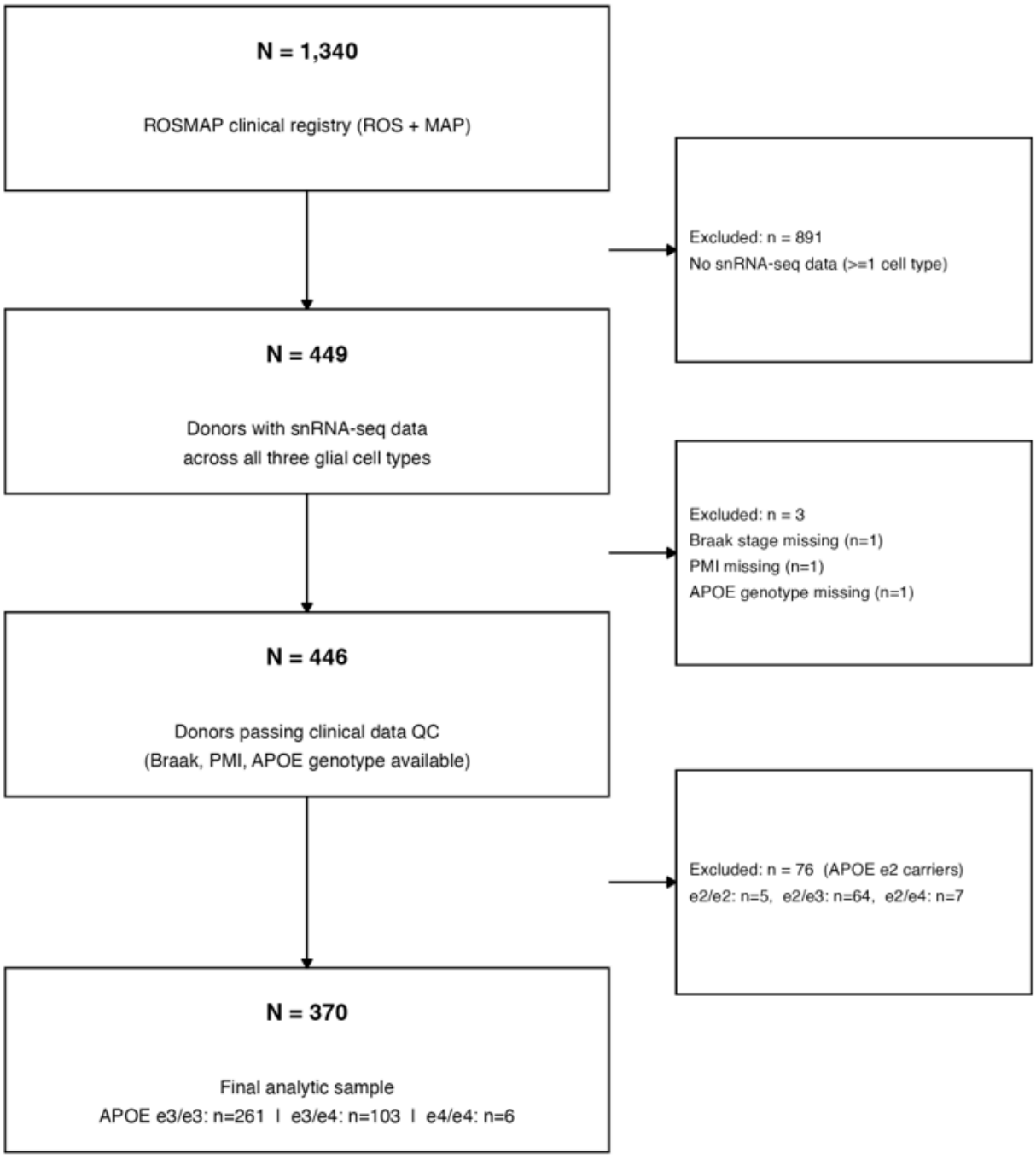
References

1. Hardy J, Selkoe DJ. The amyloid hypothesis of Alzheimer's disease: progress and problems on the road to therapeutics. science. 2002;297(5580):353-6.
2. Scheltens P, De Strooper B, Kivipelto M, Holstege H, Chételat G, Teunissen CE, et al. Alzheimer's disease. The Lancet. 2021;397(10284):1577-90.
3. Nelson PT, Alafuzoff I, Bigio EH, Bouras C, Braak H, Cairns NJ, et al. Correlation of Alzheimer disease neuropathologic changes with cognitive status: a review of the literature. Journal of Neuropathology & Experimental Neurology. 2012;71(5):362-81.
4. Smith AM, Davey K, Tsartsalis S, Khozoie C, Fancy N, Tang SS, et al. Diverse human astrocyte and microglial transcriptional responses to Alzheimer's pathology. Acta neuropathologica. 2022;143(1):75-91.
5. Pascoal TA, Benedet AL, Ashton NJ, Kang MS, Therriault J, Chamoun M, et al. Microglial activation and tau propagate jointly across Braak stages. Nature medicine. 2021;27(9):1592-9.
6. Heneka MT, Carson MJ, El Khoury J, Landreth GE, Brosseron F, Feinstein DL, et al. Neuroinflammation in Alzheimer's disease. The Lancet Neurology. 2015;14(4):388-405.
7. Keren-Shaul H, Spinrad A, Weiner A, Matcovitch-Natan O, Dvir-Szternfeld R, Ulland TK, et al. A unique microglia type associated with restricting development of Alzheimer's disease. Cell. 2017;169(7):1276-90. e17.
8. Zhou Y, Song WM, Andhey PS, Swain A, Levy T, Miller KR, et al. Human and mouse single-nucleus transcriptomics reveal TREM2-dependent and TREM2-independent cellular responses in Alzheimer's disease. Nature medicine. 2020;26(1):131-42.
9. Marschallinger J, Iram T, Zardeneta M, Lee SE, Lehallier B, Haney MS, et al. Lipid-droplet-accumulating microglia represent a dysfunctional and proinflammatory state in the aging brain. Nature neuroscience. 2020;23(2):194-208.
10. Haney MS, Pálovics R, Munson CN, Long C, Johansson PK, Yip O, et al. APOE4/4 is linked to damaging lipid droplets in Alzheimer's disease microglia. Nature. 2024;628(8006):154-61.
11. Serrano-Pozo A, Li H, Li Z, Muñoz-Castro C, Jaisa-Aad M, Healey MA, et al. Astrocyte transcriptomic changes along the spatiotemporal progression of Alzheimer's disease. Nature neuroscience. 2024;27(12):2384-400.
12. Kenigsbuch M, Bost P, Halevi S, Chang Y, Chen S, Ma Q, et al. A shared disease-associated oligodendrocyte signature among multiple CNS pathologies. Nature neuroscience. 2022;25(7):876-86.
13. Sadick JS, O'Dea MR, Hasel P, Dykstra T, Faustin A, Liddelow SA. Astrocytes and oligodendrocytes undergo subtype-specific transcriptional changes in Alzheimer's disease. Neuron. 2022;110(11):1788-805. e10.
14. Blumenfeld J, Yip O, Kim MJ, Huang Y. Cell type-specific roles of APOE4 in Alzheimer disease. Nature Reviews Neuroscience. 2024;25(2):91-110.

15. Victor MB, Leary N, Luna X, Meharena HS, Scannail AN, Bozzelli PL, et al. Lipid accumulation induced by APOE4 impairs microglial surveillance of neuronal-network activity. Cell stem cell. 2022;29(8):1197-212. e8.
16. Sienski G, Narayan P, Bonner JM, Kory N, Boland S, Arczewska AA, et al. APOE4 disrupts intracellular lipid homeostasis in human iPSC-derived glia. Science translational medicine. 2021;13(583):eaaz4564.
17. Bennett DA, Buchman AS, Boyle PA, Barnes LL, Wilson RS, Schneider JA. Religious orders study and rush memory and aging project. Journal of Alzheimer's disease. 2018;64(s1):S161-S89.
18. Olah M, Menon V, Habib N, Taga MF, Ma Y, Yung CJ, et al. Single cell RNA sequencing of human microglia uncovers a subset associated with Alzheimer's disease. Nature communications. 2020;11(1):6129.
19. Prater KE, Green KJ, Mamde S, Sun W, Cochoit A, Smith CL, et al. Human microglia show unique transcriptional changes in Alzheimer's disease. Nature Aging. 2023;3(7):894-907.
20. Mathys H, Davila-Velderrain J, Peng Z, Gao F, Mohammadi S, Young JZ, et al. Single-cell transcriptomic analysis of Alzheimer's disease. Nature. 2019;570(7761):332-7.
21. Butler A, Hoffman P, Smibert P, Papalexi E, Satija R. Integrating single-cell transcriptomic data across different conditions, technologies, and species. Nature biotechnology. 2018;36(5):411-20.
22. Hafemeister C, Satija R. Normalization and variance stabilization of single-cell RNA-seq data using regularized negative binomial regression. Genome biology. 2019;20(1):296.
23. Clarke LE, Liddelow SA, Chakraborty C, Münch AE, Heiman M, Barres BA. Normal aging induces A1-like astrocyte reactivity. Proceedings of the National Academy of Sciences. 2018;115(8):E1896-E905.
24. Loving BA, Bruce KD. Lipid and lipoprotein metabolism in microglia. Frontiers in physiology. 2020;11:393.
25. Balbo I, Montarolo F, Boda E, Tempia F, Hoxha E. Elovl5 expression in the central nervous system of the adult mouse. Frontiers in Neuroanatomy. 2021;15:669073.
26. Jung ES, Choi H, Mook-Jung I. Decoding microglial immunometabolism: a new frontier in Alzheimer's disease research. Molecular neurodegeneration. 2025;20(1):37.
27. Braak H, Braak E. Neuropathological stageing of Alzheimer-related changes. Acta neuropathologica. 1991;82(4):239-59.
28. De Jager PL, Ma Y, McCabe C, Xu J, Vardarajan BN, Felsky D, et al. A multi-omic atlas of the human frontal cortex for aging and Alzheimer's disease research. Scientific data. 2018;5(1):180142.
29. Subramanian A, Tamayo P, Mootha VK, Mukherjee S, Ebert BL, Gillette MA, et al. Gene set enrichment analysis: a knowledge-based approach for interpreting genome-wide expression profiles. Proceedings of the national academy of sciences. 2005;102(43):15545-50.
30. Korotkevich G, Sukhov V, Budin N, Shpak B, Artyomov MN, Sergushichev A. Fast gene set enrichment analysis. biorxiv. 2021:060012.

31. Liberzon A, Birger C, Thorvaldsdóttir H, Ghandi M, Mesirov JP, Tamayo P. The molecular signatures database hallmark gene set collection. Cell systems. 2015;1(6):417-25.
32. Milacic M, Beavers D, Conley P, Gong C, Gillespie M, Griss J, et al. The reactome pathway knowledgebase 2024. Nucleic acids research. 2024;52(D1):D672-D8.
33. Tingley D, Yamamoto T, Hirose K, Keele L, Imai K. Mediation: R package for causal mediation analysis. Journal of statistical software. 2014;59:1-38.
34. Nugent AA, Lin K, Van Lengerich B, Lianoglou S, Przybyla L, Davis SS, et al. TREM2 regulates microglial cholesterol metabolism upon chronic phagocytic challenge. Neuron. 2020;105(5):837-54. e9.
35. Felsky D, Roostaei T, Nho K, Risacher SL, Bradshaw EM, Petyuk V, et al. Neuropathological correlates and genetic architecture of microglial activation in elderly human brain. Nature communications. 2019;10(1):409.
36. Dias D, Portugal CC, Relvas J, Socodato R. From genetics to neuroinflammation: the impact of ApoE4 on microglial function in Alzheimer's disease. Cells. 2025;14(4):243.
37. Ahn YH, Kang JG, Choi D, Kim D-J, Yang C-M, Lee S-Y, et al. Liver–metabolic stress, apolipoprotein E ε4, and cognition and amyloid burden: findings from the Dementia Platform Korea Trial-Ready Registry. Frontiers in Aging Neuroscience.18:1773977.
38. Squair JW, Gautier M, Kathe C, Anderson MA, James ND, Hutson TH, et al. Confronting false discoveries in single-cell differential expression. Nature communications. 2021;12(1):5692.
39. Arevalo-Rodriguez I, Smailagic N, Roqué-Figuls M, Ciapponi A, Sanchez-Perez E, Giannakou A, et al. Mini-Mental State Examination (MMSE) for the early detection of dementia in people with mild cognitive impairment (MCI). Cochrane database of systematic reviews. 2021(7).

Figures



snRNA-seq = single-nucleus RNA sequencing. APOE = apolipoprotein E. PMI = post-mortem interval. Braak stage: neurofibrillary tangle staging (0-6). APOE e2 carriers excluded due to opposing biological effects of the e2 allele on lipid metabolism and AD risk.

Figure 1

Study participant selection flowchart.

From the ROSMAP clinical registry (N = 1,340), donors with single-nucleus RNA sequencing data available across all three glial cell types (microglia, astrocytes, oligodendroglia) were identified (n = 449). Following exclusion of donors with missing Braak stage (n = 1), PMI (n = 1), or APOE genotype (n = 1),

446 donors passed clinical data quality control. APOE ε2 carriers were subsequently excluded (n = 76; ε2/ε2: n = 5, ε2/ε3: n = 64, ε2/ε4: n = 7) to avoid confounding of APOE ε4 effect estimates by the opposing risk profile of the ε2 allele. The final analytic sample comprised 370 donors (APOE ε3/ε3: n = 261, ε3/ε4: n = 103, ε4/ε4: n = 6).

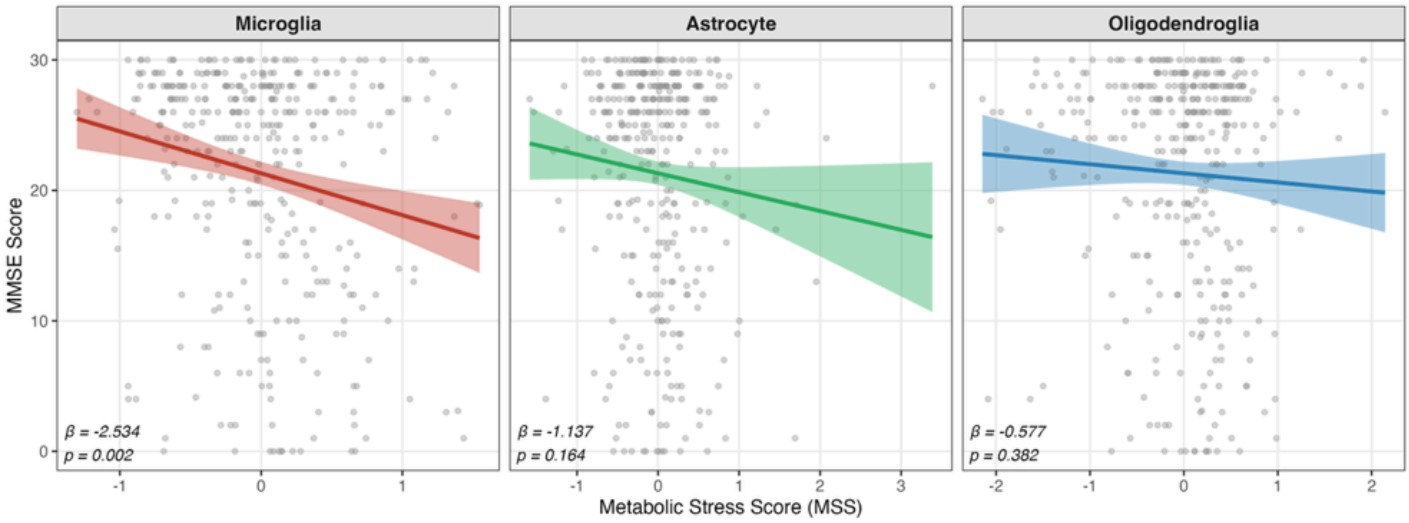


Figure 2

Cell-type-specific associations between metabolic stress score and cognitive performance.

Scatterplots depicting the association between Metabolic Stress Score (MSS) and Mini-Mental State Examination (MMSE) score for microglia (red), astrocytes (green), and oligodendroglia (blue). Each point represents one donor (n = 370). Regression lines and 95% confidence intervals are shown. Only microglial MSS was significantly associated with MMSE after adjustment for age at death, sex, postmortem interval, and APOE ε4 status (β = −2.534, p = 0.002). Astrocyte MSS (β = −1.137, p = 0.164) and oligodendroglia MSS (β = −0.577, p = 0.382) did not reach statistical significance. Regression coefficients (β) and p-values are displayed within each panel.

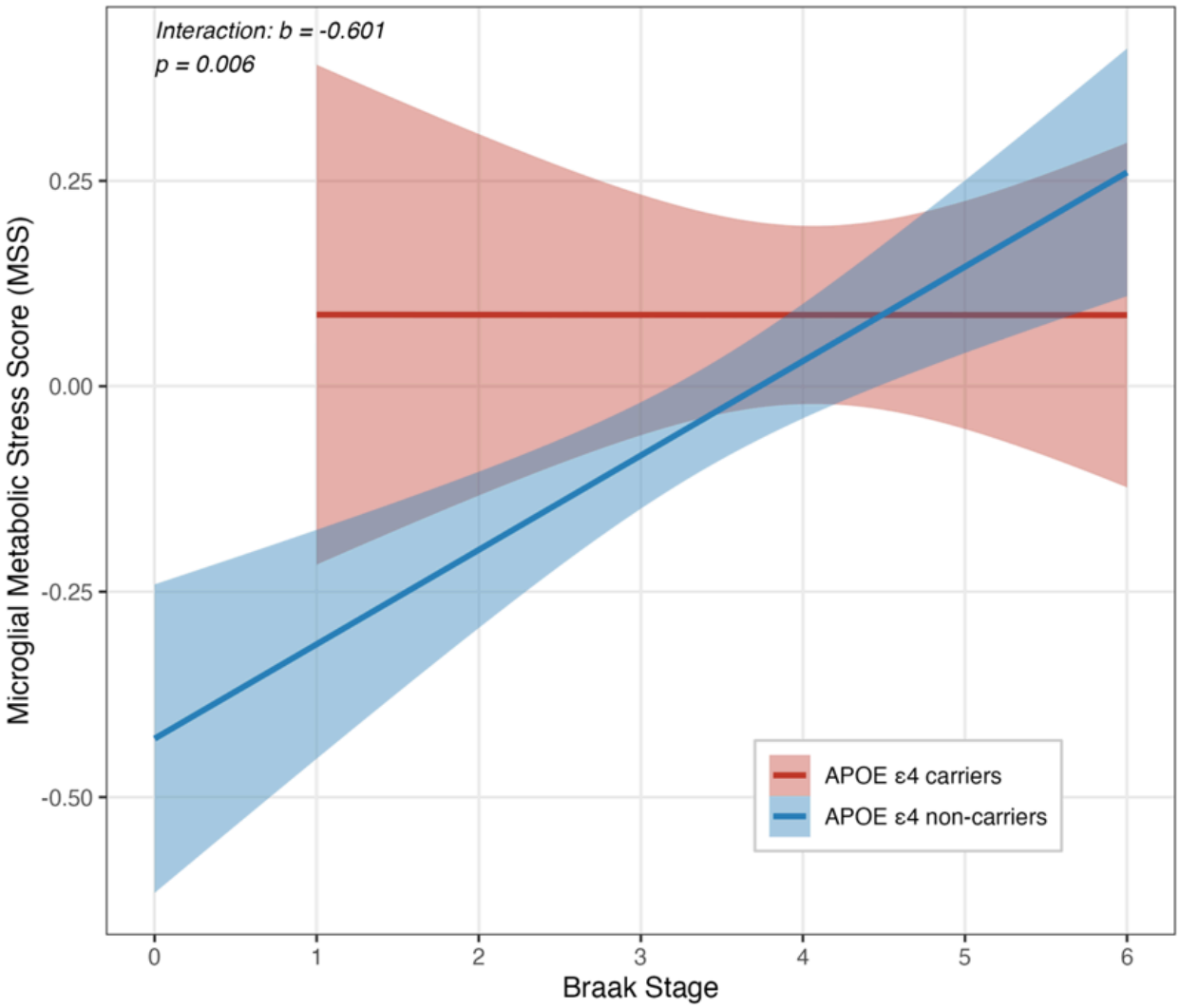


Figure 3

APOE ε4–dependent trajectories of microglial metabolic stress across Braak stages.

Linear regression–fitted trajectories of microglial MSS across Braak stages (0–6), stratified by APOE ε4 carrier status. Red: APOE ε4 carriers (n = 109); blue: APOE ε4 non-carriers (n = 261). Shaded bands represent 95% confidence intervals. A significant Braak × APOE4 interaction (β = −0.601, p = 0.006) indicates divergent trajectories across genotype groups. APOE ε4 carriers demonstrated constitutively elevated microglial MSS from early Braak stages, with mean MSS at Braak stage 1 (+0.490) comparable to levels observed in non-carriers at Braak stages 5–6. Non-carriers showed a progressive increase in MSS with advancing tau pathology. The interaction term and p-value are displayed in the upper left of the figure.

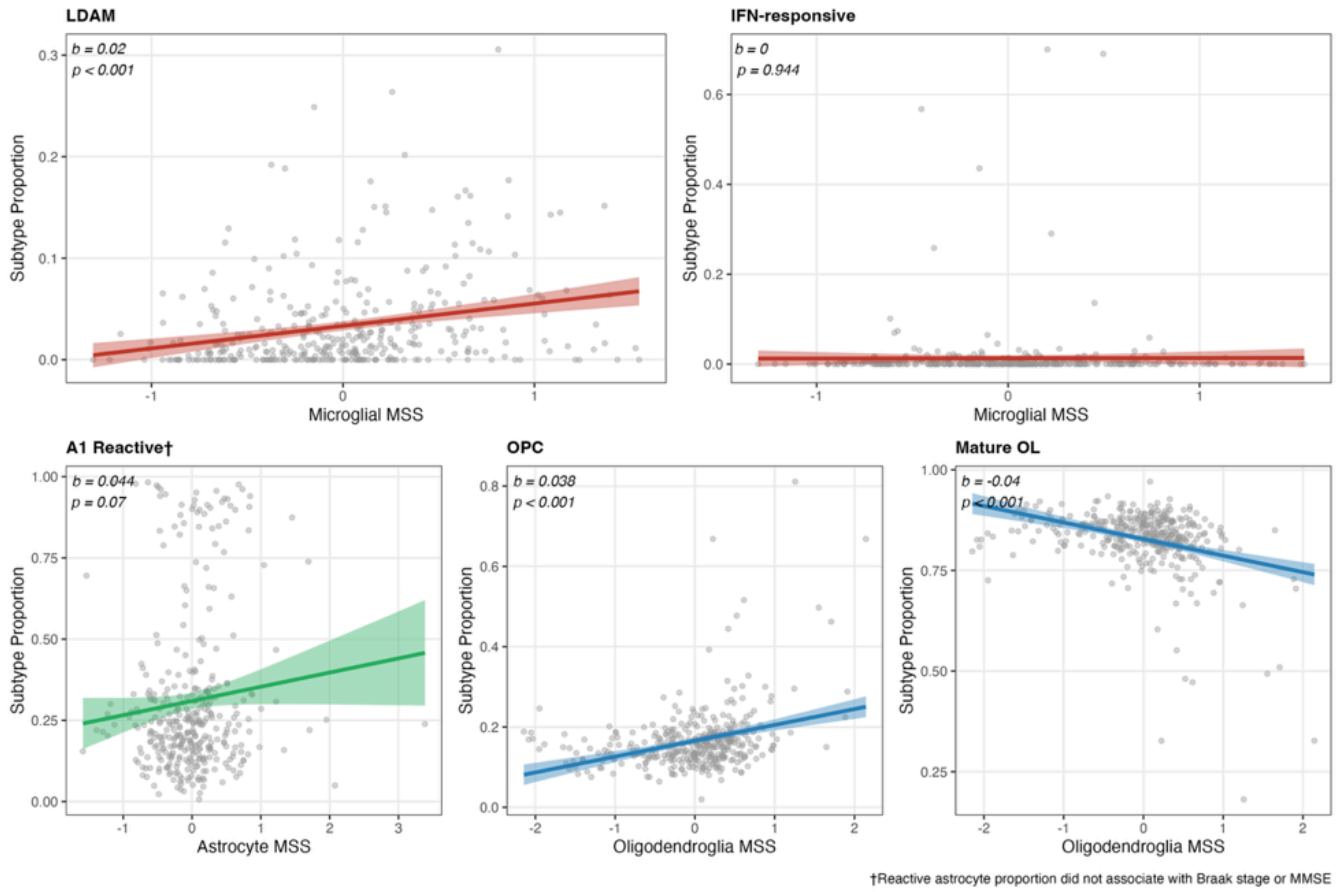


Figure 4

Glial subtype coupling to cell-type-specific metabolic stress scores.

Association between glial subtype proportions and cell-type-specific MSS across 370 donors. Upper panels: microglial subtypes — lipid-droplet associated microglia (LDAM; β = +0.019, p < 0.001) and IFN-responsive microglia (β ≈ 0, p = 0.975) plotted against microglial MSS. Lower panels: astrocyte A1 reactive subtype proportion plotted against astrocyte MSS (β = +0.043, p = 0.077†); oligodendrocyte precursor cell (OPC) proportion (β = +0.038, p < 0.001) and mature oligodendrocyte (Mature OL) proportion (β = −0.040, p < 0.001) plotted against oligodendroglia MSS. Each point represents one donor. Regression lines and 95% confidence intervals are shown. †Reactive astrocyte proportion showed a trend toward association with astrocyte MSS but did not associate with Braak stage or MMSE, suggesting a disease-independent reactive phenotype.

Supplementary Files

This is a list of supplementary files associated with this preprint. Click to download.

- SupplementaryInfromation.docx